

Efficiency of Different Chain-Linking Agents in the Synthesis of Long-Chain Branched Polypropylene: Molecular, Thermal, and Rheological Characterization

Jorge Guapacha, Enrique M. Vallés, Marcelo D. Failla & Lidia M. Quinzani

To cite this article: Jorge Guapacha, Enrique M. Vallés, Marcelo D. Failla & Lidia M. Quinzani (2017): Efficiency of Different Chain-Linking Agents in the Synthesis of Long-Chain Branched Polypropylene: Molecular, Thermal, and Rheological Characterization, Polymer-Plastics Technology and Engineering, DOI: [10.1080/03602559.2017.1373404](https://doi.org/10.1080/03602559.2017.1373404)

To link to this article: <http://dx.doi.org/10.1080/03602559.2017.1373404>



Published online: 05 Oct 2017.



Submit your article to this journal [↗](#)



View related articles [↗](#)



View Crossmark data [↗](#)



Efficiency of Different Chain-Linking Agents in the Synthesis of Long-Chain Branched Polypropylene: Molecular, Thermal, and Rheological Characterization

Jorge Guapacha^{a,b}, Enrique M. Vallés^{a,b}, Marcelo D. Failla^{a,c}, and Lidia M. Quinzani^{a,b}

^aPlanta Piloto de Ingeniería Química, UNS-CONICET, Bahía Blanca, Argentina; ^bDepartamento de Ingeniería Química, Universidad Nacional del Sur, Bahía Blanca, Argentina; ^cDepartamento de Ingeniería, Universidad Nacional del Sur, Bahía Blanca, Argentina

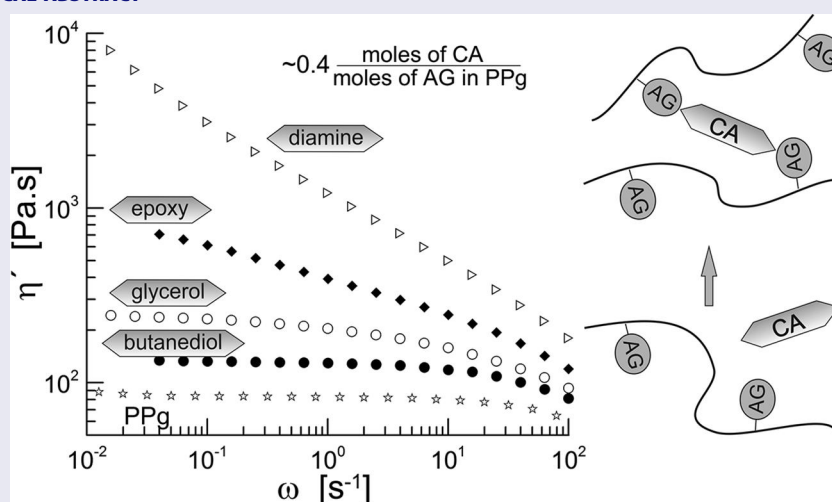
ABSTRACT

Long-chain branched polypropylenes were synthesized from a maleic anhydride grafted polypropylene (PPg). Different levels of branching were generated by reactive processing using four chain-linking agents: glycerol, 1,4-butanediol, 1,4-phenylenediamine, and the epoxy resin bisphenol-A diglycidyl ether. The results from Fourier transform infrared and size-exclusion chromatography confirm the grafting of the chain-linking agents onto grafted polypropylene and the generation of long-chain branches. In addition, the rheological and morphological results show that 1,4-phenylenediamine produces the largest increment of branching at significantly lower concentrations than the other chain-linking agents. Moreover, 1,4-phenylenediamine gives place to branched polypropylenes with narrower distribution of molecular structures.

KEYWORDS

Crosslinking; long-chain branched; polypropylene; structure–property relations

GRAPHICAL ABSTRACT



Introduction

The chemical modification of conventional isotactic polypropylene (iPP) by incorporating long-chain branches into its linear molecular structure is an efficient approach to enhance the melt strength and strain hardening of the polymer.^[1–6] This type of modification expands the range of applications of the iPP, as it improves its processability in transforming operations dominated by extensional flows, such as thermoforming, foaming, blow molding, and extrusion coating.

One way of producing long-chain branched PP (BPP) is by introducing a suitable co-monomer during the polymerization of the propylene.^[3,7–11] But BPPs can also be obtained by *post-polymerization* methods. Here the branching takes place during processing stages following the synthesis of PP. These methods are more convenient than the in situ polymerization due to their versatility and ease of being put into practice by the processing industry. They include *irradiation*,^[2,12–14] *solid-state reaction*,^[15,16] and *reactive melt processing*.^[4,6,10,17–25] In the last method, iPP is modified in the molten state in

the presence of an initiator, such as organic peroxide, with or without the addition of a polyfunctional monomer (the chain linking co-agent). The peroxide decomposes producing radicals that attack the molten iPP molecules, giving origin to macroradicals. These, in turn, may participate in recombination reactions or react with the co-agent, if present, generating BPP molecules.^[15] The *reactive melt processing* can be also applied to an already functionalized iPP, such as maleic anhydride grafted PP (PPg). In this case the polymer is modified through reactions between the functional groups of the co-agent and the grafted anhydride groups of PPg, giving place to the linkage of macromolecules. Different chain-linking agents (CA) have been used to generate BPPs, such as epoxies, diamines, polyfunctional acrylates, triallyl phosphate, vinyl silanes, butenyl styrene, hetero-aromatic derivatives, etc.^[4,6,10,18,20–22,25] Diamines,^[17,23] epoxies,^[19,26] and glycerol^[27] have also been used to modify PPg.

In previous studies, we have synthesized BPPs by reactive processing of a PPg in the molten state using glycerol and bisphenol-A diglycidyl ether as chain-linking agents.^[26,27] In this work, BPPs based on the same PPg and using 1,4-butanediol and 1,4-phenylenediamine are studied. The four families of modified PPs are also compared aiming to determine the most effective CA, that is, the CA that produces more homogenous distribution of molecular structures and similar properties with smaller concentrations of CA. Thereby, infrared spectroscopy was used to verify the occurrence of the reaction between the anhydride groups of PPg and the reactive groups of the CAs. Triple-detector size-exclusion chromatography was used to determine molecular weight distributions and to estimate the degree of branching of the BPPs. Finally, the linear viscoelastic behavior and the thermal properties of the synthesized materials were determined and analyzed as a function of the molecular structure.

Experimental

Materials

The raw material is a commercial PPg with maleic anhydride from Uniroyal Chemical (Polybond 3200, $M_w = 120 \text{ kg mol}^{-1}$ and $M_w/M_n = 2.6$). The concentration of anhydride groups (AG) in PPg estimated by FTIR is 0.74 wt%, which corresponds to the existence of a mean of ~ 4 AGs in an average PPg molecule.^[26,27] Table 1 lists the four chain-linking agents compared in this work: glycerol (from Anedra Research AG S.A), 1,4-butanediol (from Fluka Sigma-Aldrich), 1,4-phenylenediamine (from Fluka Sigma-Aldrich), and bisphenol-A diglycidyl ether (D.E.R 332 from Dow Chemical), which were used as provided.

Modification of PPg

The reactive processing of the PPg was done in a Brabender Plastograph[®] apparatus equipped with cam-blades, mixing for 15 min at 190°C under nitrogen atmosphere at 40 rpm. The so modified materials were dissolved in xylene at 120°C under constant stirring and inert atmosphere and subsequently precipitated using methyl-ethyl-ketone at 10°C to extract the unreacted CAs and secondary products that may be present. Finally, the materials were dried keeping them at 80°C under vacuum during 48 h. The BPPs are identified as PPgx – y where x is a letter that identifies the CA:G for glycerol, B for 1,4-butanediol, P for 1,4-phenylenediamine and E for the epoxy resin, and y its concentration. For example, PPgG-06 is the BPP synthesized using 0.6 wt% of glycerol.

Table 2 displays all the synthesized BPPs that are analyzed in this work and the concentration of CA used in each case. Although not included in this paper, higher concentrations of G and E have been tested given place to materials having measurable fractions of gel.^[26,27] Those BPPs from the G- and E-families

Table 1. Chemical species used as chain-linking agents.

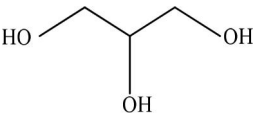
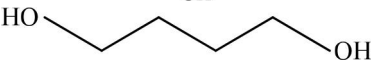
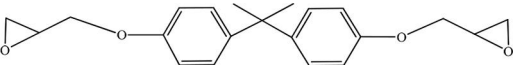
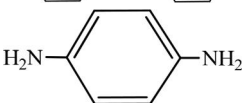
Name [ID]	Molecular structure	M (g mol^{-1})
Glycerol [G]		92.1
1,4-Butanediol [B]		90.1
Bisphenol-A diglycidyl ether [E] (RE)		340
1,4-Phenylenediamine [P]		108.1

Table 2. Synthesized materials and parameters calculated from SEC. The original PPg has $M_w = 120 \text{ kg mol}^{-1}$, $M_w/M_n = 2.6$ and 0.74 wt% of AGs.

BPP	CA (wt%)	moles CA/moles AG in PPg	AG (wt%)	M_w (kg mol ⁻¹) [PD]	N_{LCB} at...		
					3×10^5	1×10^6	$2-3 \times 10^6$
Glycerol							
G01	0.11	0.16	0.64	160 [3.1]	0	~0.2	—
G02	0.21	0.31	0.56	240 [3.4]	~0.1	~0.3	—
G03	0.31	0.45	0.42	400 [6.7]	~0.1	~0.3	~0.35
G06	0.60	0.87	0.40	(380 [5.4])	~0.3	~0.45	~0.55
Butanediol							
B03	0.28	0.41	0.54	135 [2.7]	~0.1	~0.2	—
B09	0.92	1.36	0.47	205 [2.8]	~0.2	~0.25	~0.3
B2	2.29	3.40	0.43	270 [3.5]	~0.3	~0.4	~0.45
B3	2.95	4.38	0.42	330 [3.9]	~0.45	~0.45	~0.5
B4	4.58	6.80	0.42	330 [4.7]	~0.4	~0.45	~0.6
Epoxy							
E07	0.65	0.24	0.50	175 [3.0]	~0	~0.15	~0.2
E1	1.01	0.40	0.43	515 [6.4]	~0.05	~0.4	~0.6
Phenylenediamine							
P01	0.11	0.14	0.58	150 [2.2]	~0.1	~0.2	~0.35
P02	0.21	0.27	0.48	440 [3.2]	~0.4	~0.35	~0.4
P03	0.34	0.42	0.35	(480 [2.2])	—	—	—

SEC, size-exclusion chromatography; PPg, grafted polypropylene; BPP, branched polypropylene. Molecular weight data of G06 and P03 might be affected by the filtration of a very high molecular weight tail.

considered in this work for the comparative study are those that do not present quantifiable amount of insoluble material by solvent extraction.

Characterization

Fourier transform infrared (FTIR) spectroscopy was used to analyze the presence of functional groups on BPP films of $\sim 100 \mu\text{m}$ thickness. The spectra were recorded using a Nexus spectrophotometer from Nicolet using a resolution of 4 cm^{-1} .

The molecular weight distribution of PPg and all the synthesized materials were measured using size-exclusion chromatography (SEC) with a Viscotek 350 system from Malvern. The chromatograph has three detectors: light scattering (LS), refraction index (RI), and intrinsic viscosity (IV). The chromatograms were obtained at 135°C using a set of PLgel columns ($10 \mu\text{m}$ Mixed-B LS from Polymer Labs). Trichlorobenzene containing 0.1 wt% of butyl hydroxyl toluene was used as solvent. The system was calibrated with standards of polystyrene (from Viscotek) of 98.0 and 228.2 kg/mol.

The elastic and viscous moduli of all materials were determined using an AR-G2 rheometer from TA instruments with parallel plates of 25 mm in diameter. The samples, 25 mm diameter disks with a thickness of 2 mm, were prepared by compression at 180°C , and analyzed under small-amplitude oscillatory shear flow. Dynamic frequency sweeps were performed in the range $0.01-100 \text{ s}^{-1}$ in the stress-controlled mode using a constant shear stress of 10 Pa. This value, which was determined beforehand from dynamic stress sweeps applied to all materials, guarantees that the dynamic tests are

performed in the linear viscoelastic regime. Temperatures between 170 and 200°C were considered.

Finally, the thermal behavior of the polymers was analyzed using a Pyris 1 calorimeter from PerkinElmer Co. under nitrogen flow. The tests were started heating the samples up to 180°C and keeping them 3 min at this temperature to erase their thermal history. Then, they were cooled down up to room temperature (cooling rates of 2.5, 5, 10, and $20^\circ\text{C min}^{-1}$), and finally heated back up to 180°C (at $10^\circ\text{C min}^{-1}$).

Results and discussion

Structure characterization

The chain-linking process of PP implies that the raw material, PPg, changes its structure due to the reaction of the AGs with the reactive groups of the CAs (amine, hydroxyl, and oxyrane groups). These reactions produce new chemical groups, such as ester and amide, according to reaction mechanisms which have already been proposed in the literature.^[19,23,28] Thus, a larger amount of CA should produce a larger decline of the concentration of AGs and a larger increase of that of the new groups. Moreover, since all CA have at least two functional groups, the reaction between PPg and the CAs should give place to chain-linking between neighboring macromolecules.

The reaction among PPg and the different CAs was verified by FTIR analyzing the evolution of the absorbance of the anhydride, ester, and imide groups. As an example, Figure 1 displays two regions of the FTIR spectra of PPg and some BPPs. One BPP of each family has been selected, being representative of the behavior

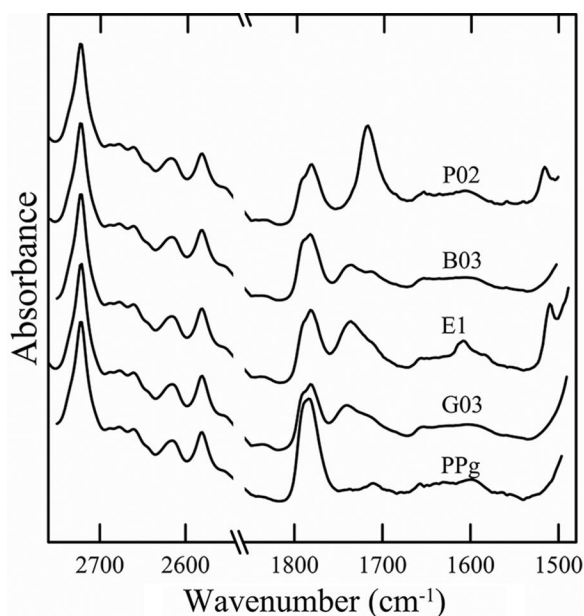


Figure 1. FTIR spectra of PPg and one modified polymer from each family of BPPs. Note: FTIR, Fourier transform infrared; PPg, grafted polypropylene; BPP, branched polypropylene.

of each family of polymers. Those selected have similar molar concentration of CA to original AGs (a molar ratio of approximately 0.4). The spectra have been normalized with the absorbance band of the methine group of the PP backbone at $2,720\text{ cm}^{-1}$ ^[29] and shifted arbitrarily in the y -axis. The region of the spectra that includes this absorbance band is shown at the left in Figure 1. At the right, the region of the spectra that includes the absorbance bands associated to carbonyl and aromatic groups is shown. The spectra of PPg shows significant absorption bands at $1,792$ and $1,860\text{ cm}^{-1}$, associated to the stretching of the C=O group of the anhydride. These bands also appear in the spectra of all BPPs although with less intensity. The G-, B-, and E-families of BPPs display absorbance bands at $1,715$ and $1,735\text{ cm}^{-1}$ corresponding to the carbonyls of acid and ester groups, respectively, which appear as a consequence of the reaction between anhydride and OH groups. At $1,510$ and $1,610\text{ cm}^{-1}$ the absorbance bands of aromatic rings can be visualized in the case of the E- and P-families. In addition, the P-family displays a band centered at $1,717\text{ cm}^{-1}$ corresponding to imide groups.^[29] The reaction of AGs with amines should result in amide and acid groups, which react producing imides.^[23,30,31] The lack of absorbance bands at $3,300$ – $3,500$ and $1,680$ – $1,690\text{ cm}^{-1}$ in the spectra of the P-family, which correspond to amine and amide groups, respectively, indicates that the amount of these groups that may subsists after the reaction is insignificant. The absorbance bands of the anhydride,

ester, acid, and imide in the spectra of the BPPs change with the extension of the reaction as will be analyzed further down.

The amount of anhydrides in each material was computed using the normalized absorbance of the band at $1,792\text{ cm}^{-1}$ (A_{1792}/A_{2720}) and the calibration curve:

$$\frac{A_{1792}}{A_{2720}} = 1.30 \times \text{wt\% AG} \quad (1)$$

This curve was obtained measuring the absorbances of physical mixtures of PP and succinic anhydride.^[27] The concentration of AG in each polymer was determined using this equation. The values are listed in Table 2. These values are also plotted in Figure 2 as a function of the ratio of the molar concentration of CA used in the modification with respect to that of AG in PPg (m_{CA}/m_{AG}). The value calculated for PPg, 0.74 wt%, also determined with this equation, is located in the y -axis ($m_{CA}/m_{AG} = 0$). As expected, the concentration of AGs decreases from this value in the four families of polymers with the addition of CA. However, it can also be appreciated that in the B- and G-families, for m_{CA}/m_{AG} higher than 0.5, there is a change in behavior. The amount of AGs in the BPPs in this range decreases very slowly as m_{CA}/m_{AG} increases. The same was observed for larger concentrations of G and E as discussed in previous works.^[26,27] It is interesting to notice that the reduction from 0.74 to ~ 0.5 wt% of

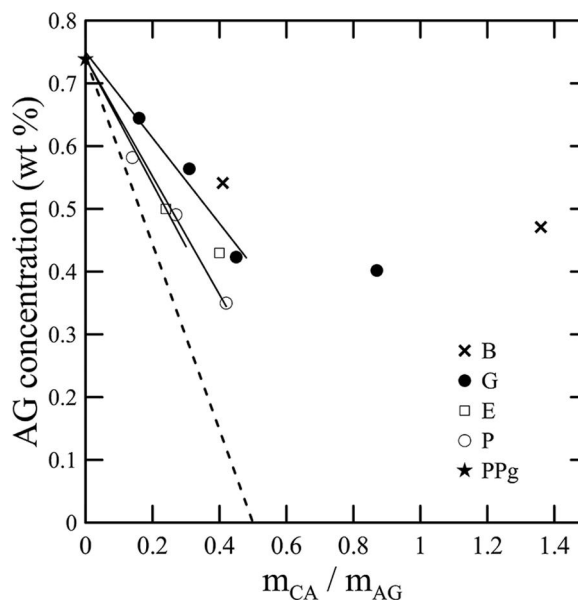


Figure 2. Concentration of AG of the polymers as a function of the molar concentration of CA relative to the molar concentration of AGs in PPg. Full-lines correspond to the linear fit of the data at low concentrations, while the dashed-line represents the situation in which each mole of CA reacts with two moles of AG. Note: PPg, grafted polypropylene.

AG corresponds to the disappearance of approximately two AGs every two average PPg molecules (with 3.6 AG per molecule) which suggest that the reaction begins homogeneously in all the bulk. Then, B, as it happens with G and E, displays a limit concentration (at $m_{CA}/m_{AG} \sim 0.5$) above which the functional groups do not have possibility of getting near the AGs to react. This behavior may be due to phase separation of these CA at large concentrations and/or to lack of accessibility to the AGs still present in the modified PPg molecules. It should also be mentioned that, as expected, the concentration of the chemical groups generated in each case from the reaction of the CA and the AGs, significantly augment at low concentrations of m_{CA}/m_{AG} opposing the behavior of AGs, and change slowly after $m_{CA}/m_{AG} \approx 0.5$. It is interesting to notice that all materials that have more than ~ 0.45 wt% of remaining AGs (which represents $\sim 60\%$ of the initial concentration in PPg) do not exhibit evidence of insoluble material. In the case of B, this occurs at all concentrations of CA. All together, these results demonstrate that the 1,4-butanediol is the less efficient of the four analyzed CAs. The behavior of this agent may be justified by a poorer solubility in the PPg bulk.

The rapid decrease of the concentration of AGs at low doses of CA can be linearly fitted (at least in the case of G, E, and P). The slopes calculated are -0.67 , -1.0 , and -0.94 for G, E, and P, respectively. The theoretical behavior in which 1 mol of CA (with a functionality of 2) reacts with 2 mol of AGs (consuming all functional groups of the added CA) is described by the dashed-line included in Figure 2, which corresponds to the equation: $\text{wt\% of AG} = 0.74 - 1.48 \times m_{CA}/m_{AG}$. As it can be observed, the four systems have slopes lower than -1.48 . In the best of the cases, just two of every three present functional groups react with AGs. Comparing G with P, both have linear behavior in the same range (m_{CA}/m_{AG} near 0.5) but the last one is more efficient, having larger slope than G although this CA has three functional groups. Similarly, comparing E with P, it is observed that both have similar values of slope but the linear behavior in the case of P extends in a larger range of CA concentration. Altogether, the FTIR analysis suggests that P is the more efficient chain-linking agent.

The polymers were also characterized using SEC with RI, LS, and IV detectors as already mentioned. Figure 3 displays the molecular weight distributions of all materials considered in this work. The curve of PPg was obtained using $dn/dc = 0.098 \text{ ml g}^{-1}$, value that was calculated for complete mass recovery. This value was then used to obtain the molecular weight distributions of all BPPs, although it is possible that it is not the

correct one since it may vary as the chemical structure of the polymer changes. Using this value, the mass recovery estimated by the technique is practically 100% in all cases. PPg exhibits a typical distribution of a polymer with a narrow unimodal distribution of molecular weights. The chromatogram also shows the presence of a fraction of very low molecular weight, below 10^4 g mol^{-1} . In general, the curves corresponding to the BPPs show a broadening of the distribution of molecular weights with a shift to larger values. This behavior is the expected one for the chain-linking process that occurs during the modification of PPg.

In the case of the G- and B-families, the position of the maximum of the distribution practically does not change with the augment in CA concentration. The decrease in concentration of low molecular weight species with the amount of CA goes together with the appearance of a tail of large molecular weight, larger than $6 \times 10^5 \text{ g mol}^{-1}$, not present in the original PPg. In the case of the E-family, E07 has the same qualitative behavior just described while E1 displays a slight shift of the maximum to higher molecular weights. The family of BPPs that display a different qualitative behavior is the one based on P. The curve of P01 is like those of the other families for small concentrations of CA. However, the use of double and triple concentrations of P gives place to important shifts in the molecular weight distributions, with the disappearance of molecules up to $\sim 5 \times 10^4 \text{ g mol}^{-1}$ in the case of P03. The shape of the distributions of these two polymers at high molecular weights, together with the decrease of the population at low molecular weights in P03, suggests that a fraction of this material may have been filtered by the system. The rheological data that will be analyzed further down sustain this result. A similar behavior was observed by El-Mabrouk et al.^[4] while modifying a PPg with tris(2-aminoethyl)amine.

The previous comments are reflected in the values of weight-average molecular weight (M_w) and polydispersity (PD) calculated from the distributions, which are listed in Table 2. It can be observed that P03 has a M_w similar to that of P02 with a lower PD, which is even lower than that of PPg. This outcome, together with the analyzed shape of the chromatogram strongly suggests the existence of very high molecular weight material in P03 that has been filtered by the SEC system. Furthermore, the decrease in the value of M_w of G06 and the slight increase of this parameter in B4, indicates that a high molecular weight fraction may exist in these polymers that may have also been retained by the filtration system. It is also interesting to notice that P01 and P02 have polydispersities similar to that of PPg. This suggest that all molecules of PPg,

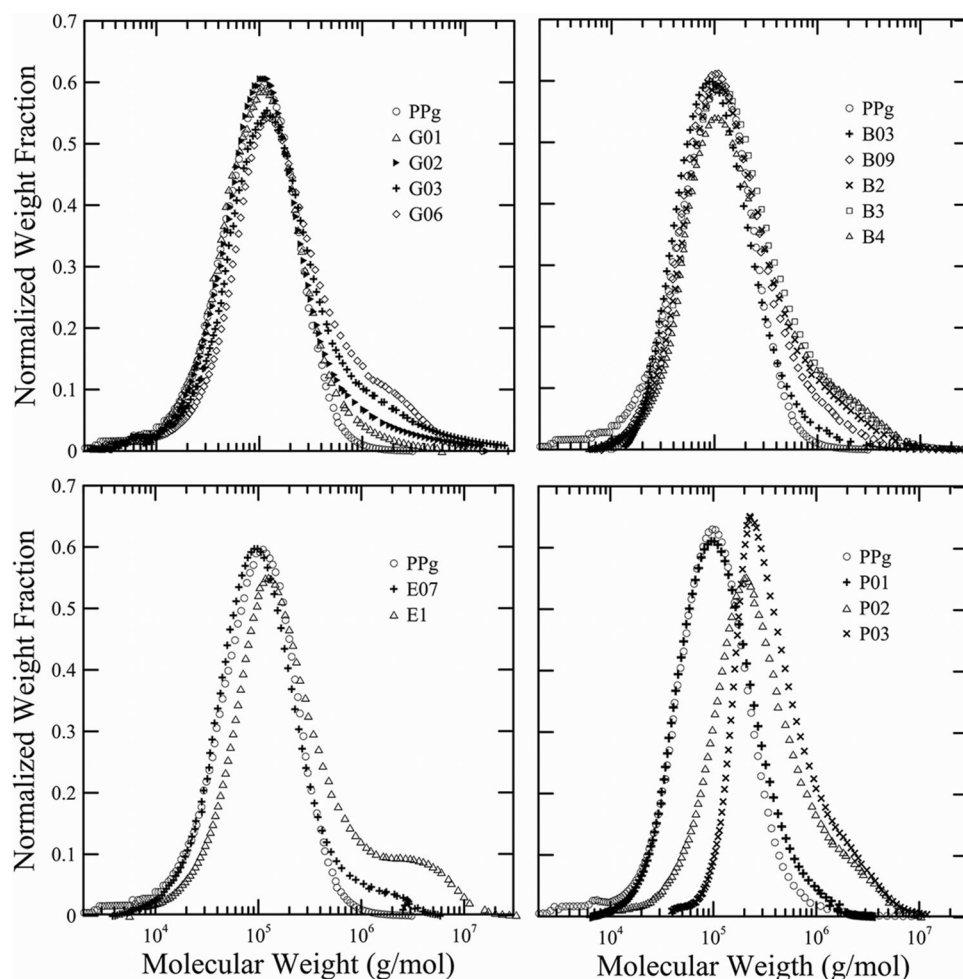


Figure 3. Normalized molecular weight distribution of all materials calculated using SEC with RI, LS and IV detectors. *Note:* SEC, size-exclusion chromatography.

independently of their size, have similar chance of reacting in the presence of P, and that this CA must be well dispersed in the bulk, at least in the range of concentrations considered. This conclusion supports the FTIR results. Both techniques indicate that 1,4-phenylenediamine is the most efficient CA producing the largest change in PPg (largest decrease in AG and shift of the molecular weight distribution to larger molecular weights) for a given concentration (at least up to $m_{CA}/m_{AG} \approx 0.5$).

Size-exclusion chromatography with multiple detectors allows measuring the intrinsic viscosity of the polymers, which can be used to characterize their molecular structure. Figure 4 displays the intrinsic viscosity data, $[\eta]$, of the polymers as a function of molecular weight. The curve of P03 is not included since, as already commented, it would not represent the whole distribution of large and complex generated structures. The prediction of the Mark–Houwink relation, $[\eta] = KM^a$, is also included in Figure 4 (solid line). This relation is expected to hold in the case of

linear polymers. The values of K and a , obtained from the fitting of the PPg data ($K = 1.74 \times 10^{-4}$ and $a = 0.69$), are very close to those reported in the literature for linear PP.^[3,32] The intrinsic viscosity data of all BPPs deviate from the Mark–Houwink relation at high molecular weights indicating the existence of branched material in all of them. Up to $2\text{--}3 \times 10^5 \text{ g mol}^{-1}$, all BPPs display a behavior not far from that of a linear material, with a change in slope as the polymer becomes more modified. Above the mentioned molecular weight, the data deviate noticeably from the Mark–Houwink relation, and extend up to larger molecular weights than those of PPg. This behavior corresponds to the existence of molecules in the BPPs that, for a given molecular weight, have smaller hydrodynamic volume than those of the linear material. These are the generated branched macromolecules, which have smaller radius of gyration than linear molecules of the same molecular mass.^[3,4] Furthermore, the progressive departure from the Mark–Houwink relation as the concentration of CA increases indicates that the complexity of the generated structures

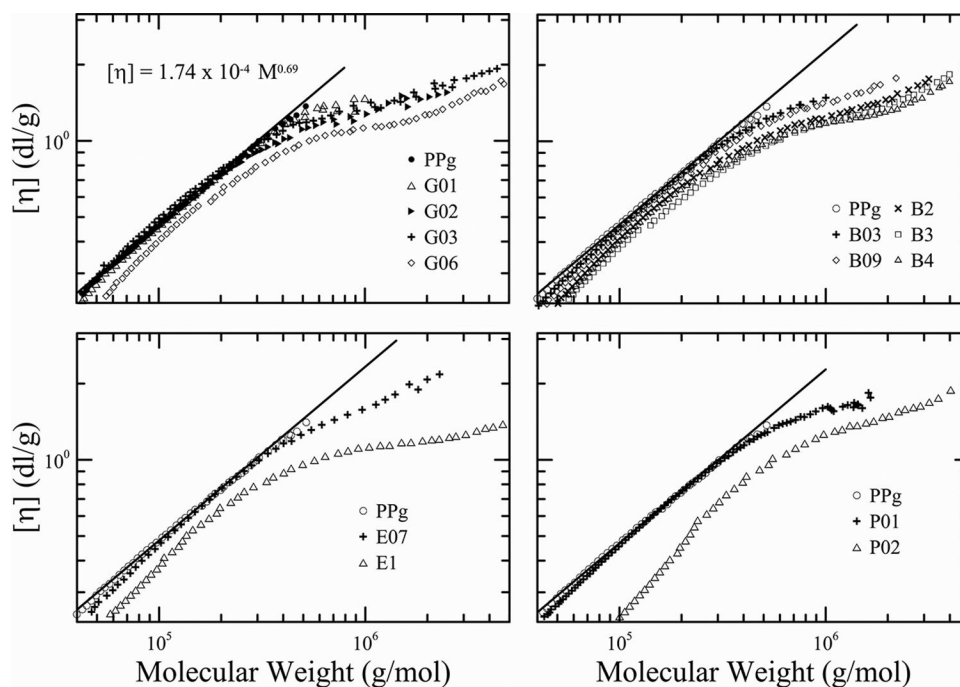


Figure 4. Intrinsic viscosity as a function of molecular weight.

augmentations. In the case of P03 (and may be G06, and even B04) the data may reflect the structure of just the soluble material.

The data of intrinsic viscosity can then be used to estimate a degree of complexity in the polymer molecules using the theory of Zimm and Stockmayer with the method of Lecacheaux.^[6,26,27,33–35] This model proposes that the ratio between the mean square radius of gyration of branched and linear molecules, g , relates with the ratio of the intrinsic viscosity of these two type of polymers, g' , through $g' = g^\varepsilon$. The parameter ε , which depends on the type of branched structure and the solvent–polymer interaction, takes values between 0.5 and 1.5. For random branched structures, a value of 0.75 is typically used^[10,24,36,37] and has been adopted in this work. Following the theory, the branching index N_{LCB} , that gives an average number of branches per 1,000 monomer units, can be calculated from

$$N_{LCB} = 1,000 \times M_M \times \frac{m}{M} \quad (2)$$

where M_M is the molecular weight of a monomer unit (42 g mol^{-1}), M the molecular weight of the polymer, and m an average number of branches per molecule, calculated from:

$$g = \frac{6}{m} \left[\frac{1}{2} \left(\frac{2+m}{m} \right)^{0.5} \ln \left(\frac{(2+m)^{0.5} + m^{0.5}}{(2+m)^{0.5} - m^{0.5}} \right) - 1 \right] \quad (3)$$

Table 2 lists the values of N_{LCB} calculated using the equations above applied to the data at three molecular weights. As expected, the branching index augments with molecular weight. Moreover, for similar values of m_{CA}/m_{AG} , the CA that produces the largest branching index is P and the one that produces the smallest is B. A value of $N_{LCB} = 0.4$ corresponds to two branches every 10^4 backbone carbons. Although this value is just indicative, since it represents a distribution of structures that may exist at a given molecular weight, it signals the existence of a large degree of branching and complexity in the generated high molecular weight molecules. Similar values of branching levels have been estimated by other authors for BPPs synthesized using different systems.^[3,6,8,12,36,38,39]

Linear viscoelastic characterization

Figures 5 and 6 display the elastic modulus (G') and the dynamic viscosity ($\eta' = G''/\omega$) of PPg and the synthesized polymers at 180°C . The linear structure of PPg molecules and the relatively low molecular weight are reflected in the dynamic parameters of this polymer. It can be seen for example that, in the terminal region, G' and G'' of PPg are practically proportional to ω^2 and ω , respectively. The BPPs present larger dynamic parameters than PPg, which increase with CA concentration, being the increment larger in G' and at low frequencies. This behavior is in accordance with the changes in structure and increase in molecular

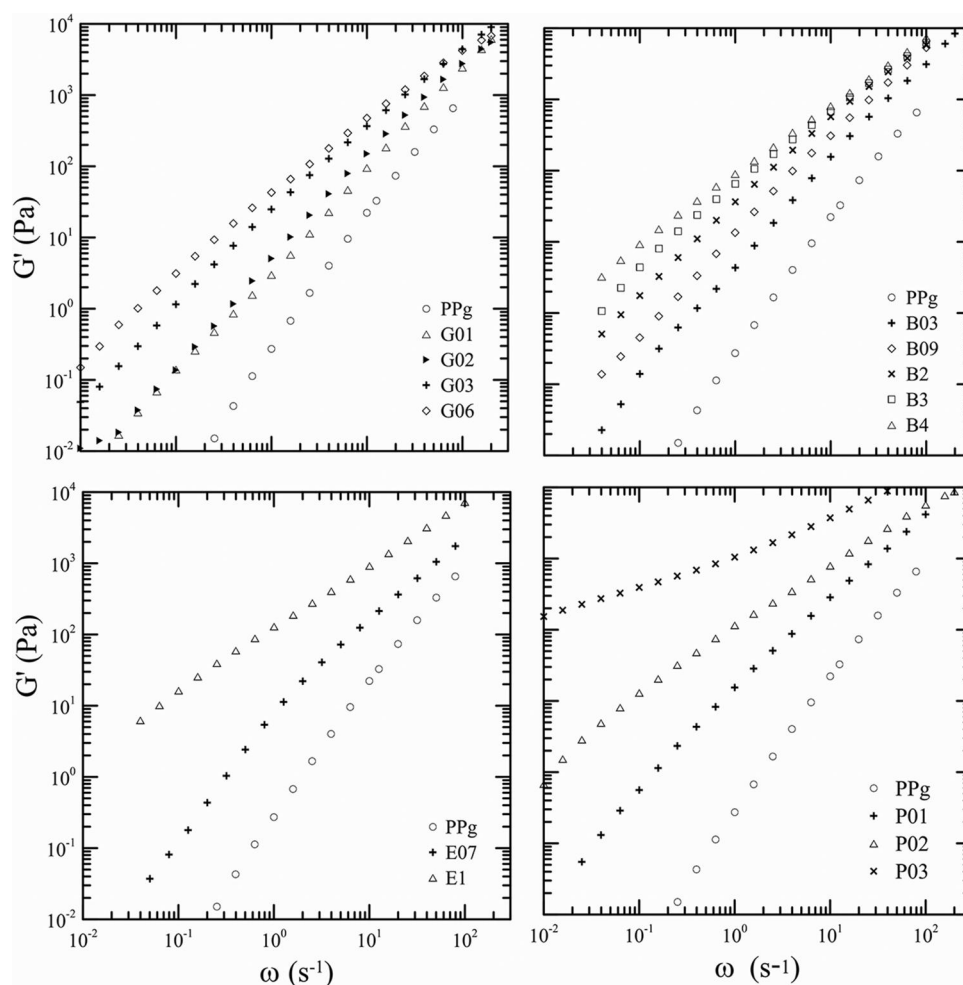


Figure 5. Elastic modulus of the polymers at 180°C as a function of frequency.

weight detected by SEC. At low frequencies, the dynamic response of a material is dominated by the slower relaxation processes (larger relaxation times) associated to the reptation movement of whole molecules and complex structures.^[40,41] However, at high frequencies, the flow becomes dominated by faster relaxation processes that correspond to smaller molecular structures (small molecules and/or molecular segments), which should be similar in all BPPs. In particular, the dynamic viscosity, display a shift from the terminal to the power law region toward higher frequencies with a loss of the Newtonian plateau in the covered frequency range. This behavior can be also attributed to the existence of branched and complex molecular structures and the influence of their longer relaxation times.^[1–4,8,12,20–22,37,39,41–43]

The results in **Figures 5** and **6** also show that, for a given m_{CA}/m_{AG} , P produces the largest augment of the dynamic moduli and B the smallest. For example, for $m_{CA}/m_{AG} \cong 0.4$, the ratio of G'_{BPP}/G'_{PPg} at $\omega = 0.04 \text{ s}^{-1}$ is 1.2×10^6 , 2.4×10^4 , 1.2×10^3 , and

8.8×10^1 for P03, E1, G03, and B03, respectively. The elastic modulus of PPg used for these comparative calculations was extrapolated as 0.00025 Pa. Similarly, η'_{BPP}/η'_{PPg} at $\omega = 0.04 \text{ s}^{-1}$ of the same polymers takes a value of 57, 8.3, 2.9, and 1.5, respectively. Accordingly, it can be concluded that, to synthesize materials with similar viscoelastic properties, the molar concentration of CA (m_{CA}) needed are: $m_B > m_G > m_E > m_P$. For example, it can be estimated that, to obtain an elastic modulus of 1 Pa at $\omega = 0.04 \text{ s}^{-1}$, the concentrations of B, G, E, and P needed are approximately 4.5, 0.9, 0.3, and 0.22 moles per mol of AG in PPg, respectively. This analysis reflects the large effect that the chain-linking process has on the rheological behavior of the BPPs, mainly in their elasticity. Furthermore, the results also confirm that phenylenediamine is the most effective CA.

The viscosity data presented in **Figure 6** also show that an inflexion point appears in the data of the BPPs at intermediate frequencies, which becomes gradually more noticeable as the CA concentration augments. This behavior has already been observed in branched

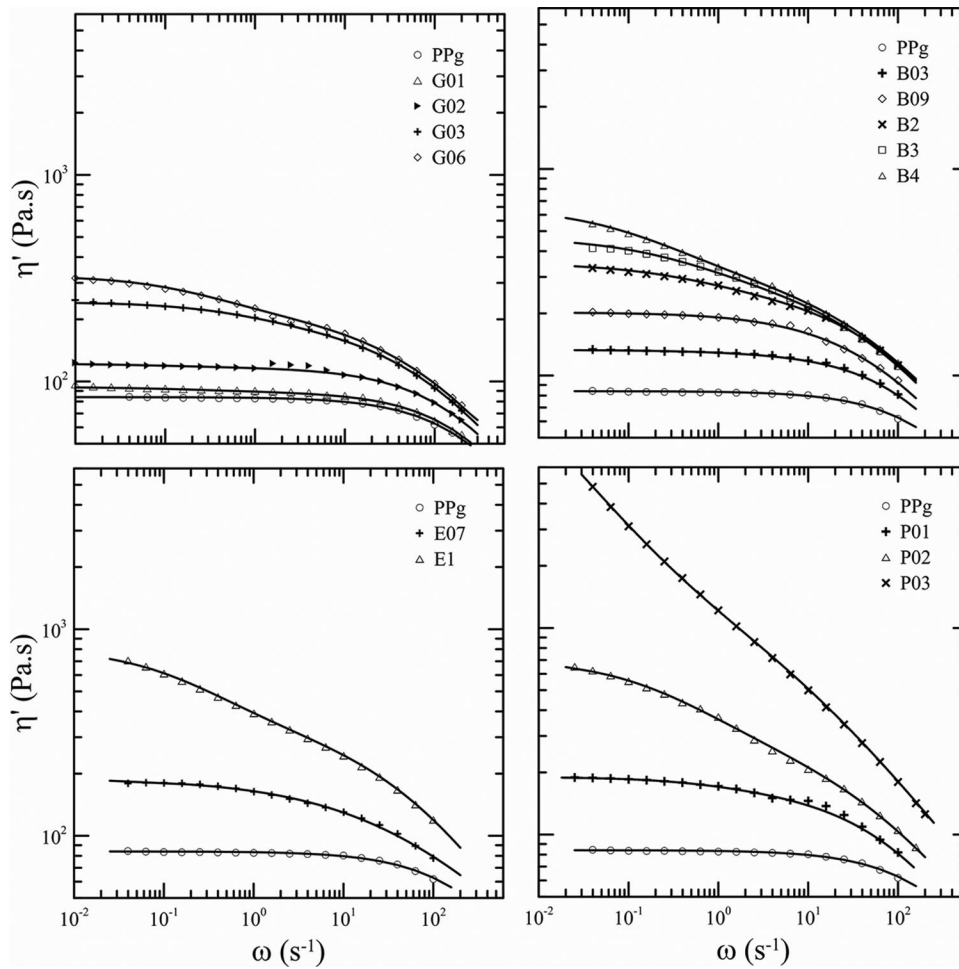


Figure 6. Dynamic viscosity of the polymers at 180°C as a function of frequency and predictions of the two-mode cross model (solid lines).

materials obtained from PP or other polymers,^[1,13,44] and it may be associated with the existence of two distinctive populations of molecules with different dominating relaxation modes. To quantify the importance of each population in the rheological behavior of the polymers, the data were modeled using a two-mode Cross model^[26,27,40]:

$$\eta'(\omega) = \frac{\eta_H}{1 + (\lambda_H \omega)^{n_H}} + \frac{\eta_L}{1 + (\lambda_L \omega)^{n_L}} \quad (4)$$

The subscripts H and L in this equation stand for high and low range of frequencies, respectively, and η_i , λ_i , and n_i are the zero-shear-rate viscosity, characteristic relaxation time, and shear-thinning index of each mode, respectively. The zero-shear-rate viscosity of each fluid predicted by this model would be $\eta_L + \eta_H$. The parameters calculated by minimum square fitting of the data in Figure 6 to Eq. (4) are listed in Table 3. In the case of G01, G02, and B03, where the inflexion point is practically inexistent, the data at $\omega > 10 \text{ s}^{-1}$ were first fitted to calculate $\{\eta_H, \lambda_H\}$ and then the value

of η_L was determined as the difference between the viscosity at small frequencies and η_H . This procedure proves the existence of a second mode (with a longer relaxation time associated) although with very small weight ($\eta_L \ll \eta_H$). The value of λ_L of G01, G02, and B03, shown in parenthesis in Table 3, are the ones used to calculate the curves in Figure 6 but were not obtained by minimum-square fitting.

In all families, the BPPs obtained with the lower doses of the different CAs have characteristic relaxation times at high frequencies (λ_H) that are not far from the terminal relaxation time of PPg (0.0026 s), and that increase moderately with the concentration of CA. Moreover, the importance of this mode, which is given by the viscosity parameter, η_H , does not change markedly from one polymer to the other, being at most three times larger than $\eta_{0,PPg}$. P03 is an exception due to the large degree of modification reached in this case. Moreover, the shape of the dynamic viscosity curve of P03 suggests the existence of a yield stress, which is another evidence of the presence of a fraction of very large and

Table 3. Parameters obtained by fitting the two-mode cross model to the data in Figure 6.

	η_H (Pa · s)	λ_H (s)	n_H	η_L (Pa · s)	λ_L (s)	n_L	$\eta_H + \eta_L$ (Pa · s)
PPg	84	0.0026	~0.8	—	—	—	84
G01	89	0.0028	0.8	4	(0.5)	(0.8)	94
G02	117	0.0038	0.75	5	(0.5)	(0.8)	122
G03	184	0.010	0.64	58	1.1	0.8	242
G06	205	0.012	0.62	120	3.5	0.8	325
B03	128	0.0052	0.77	5	(0.5)	(0.8)	133
B09	140	0.008	0.70	62	0.4	0.7	202
B2	235	0.012	0.68	115	1.6	0.7	350
B3	255	0.017	0.63	210	2.2	0.8	465
B4	280	0.020	0.60	370	6.0	0.7	650
E07	145	0.009	0.70	38	0.77	0.8	183
E1	300	0.023	0.60	570	7.0	0.7	870
P01	160	0.010	0.70	30	0.8	(0.8)	190
P02	240	0.020	0.60	470	3.3	0.7	710
P03	950	0.20	0.55	35000	600	0.65	35950

complex molecules. The second mode, which corresponds to the low frequency range, presents relaxation times (λ_L) that are at ~ 2 orders of magnitude larger than λ_H , which also increase with CA concentration. Moreover, it can be observed that this mode, which reflects the dynamic of the large molecular structures, is unimportant in the case of BPPs slightly branched (see value of η_L) but increases rapidly in importance as the concentration of CA augments.

The previous comments are illustrated in Figure 7, which displays the ratios λ_L/λ_H and η_L/η_H as a function of m_{CA}/m_{AG} . This figure includes the data of three BPPs obtained with larger doses of G or E, which present fractions of gel-like material and were part of the analysis in previous works.^[26,27] They are included to assist in the comparative analysis of the BPPs families. The value of λ_L/λ_H demonstrates that the new populations of macromolecules have complex structures with much longer relaxation times. The value of the ratio η_L/η_H , however, shows that the long time relaxation process practically

does not contribute to the dynamic of the whole system at low doses of CA but becomes increasingly significant as the concentration of CA augments. In fact, this mode dominates in B4, E1, P02, and P03 (when $\eta_L/\eta_H > 1$). The data in Figure 7 also emphasize the importance of the type of CA used in the modification process. For example, if the comparison is done at a given m_{CA}/m_{AG} (like ~ 0.4), the relaxation mode of the new complex molecular structures is obviously much important for the diamine than for the rest of the CAs, being followed by the epoxy, then the glycerol and finally the diol.

Moreover, it can be observed that the relative importance of the relaxation process associated to the new complex structures with respect to the smaller or simpler ones (η_L/η_H) is much larger in the P-family (soluble materials) than in BPPs than contain measurable fractions of gel-like material (data in empty symbols in Figure 7 corresponding to the G- and E-families). For a polymer with a fraction of gel-like material to have

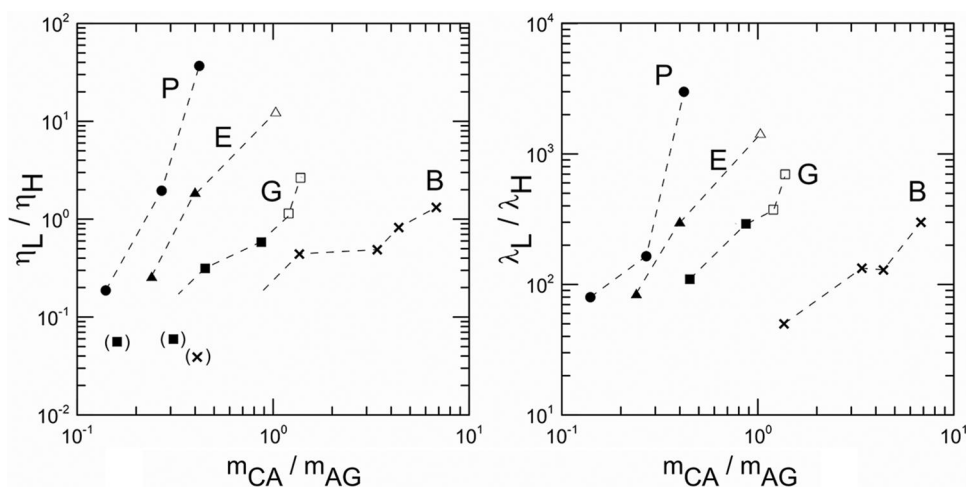


Figure 7. Ratios of the viscosity and relaxation time parameters of the two-mode cross model (see Table 3) as a function of the molar concentration of CA relative to the molar concentration of AGs in PPg. Data between parenthesis have lower precision. Data signaled with empty symbols correspond to materials discussed in Guapacha et al.^[26,27]

smaller relative viscosity at small frequencies, it has to include a fraction of small or much simpler molecules that act diluting the large ones. By comparison, the BPPs of the P-family should have more homogeneous distributions of molecular structures. This agrees and reinforces the conclusion from the structural characterization, in the sense that phenylenediamine is the most efficient chain-linking agent, reaching a more homogeneous distribution in the PPg bulk than the other CAs and, consequently, giving place to BPPs more uniformly modified.

The complexity in molecular structure also reflects in the thermorheological behavior. Normally, polymers based on molecules of linear structure are thermorheologically simple, which means that the Time-Temperature Superposition Principle can be used to produce master curves of the rheological parameters. Long-chain branched materials, even those with very low branching level, fail in the application of this principle.^[26,27,40,41,43,45] In this study, PPg was the only material that displayed thermorheologically simple behavior. All BPPs, even the ones obtained with the lower doses of CA had complex behavior. As an example, Figure 8 displays the master curves of the phase angle, $\delta = \tan^{-1}(G''/G')$, of PPg and selected BPPs (G02, B03, E07, and P01) obtained with low concentrations of CA. The curves were built from data obtained between 170 and 200°C, being 180°C the reference temperature. In the case of PPg, the phase angle data measured at each temperature were shifted along the x -axis up to superposition with those at 180°C. At each

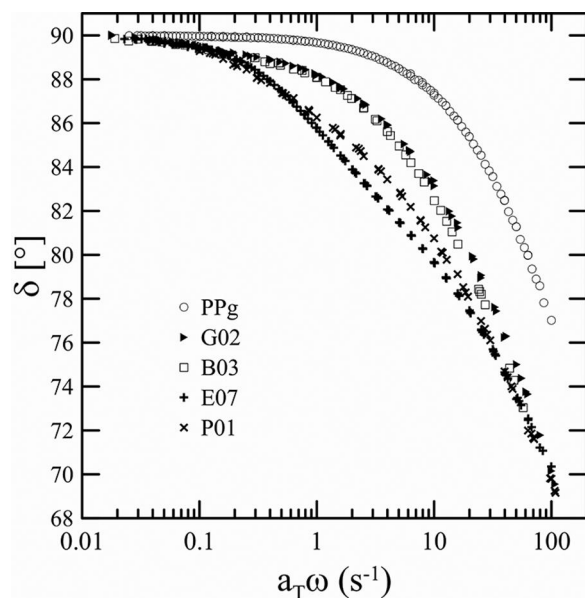


Figure 8. Master curves of the phase angle of PPg, G02, B03, P01, and E07. $T_{ref} = 180^\circ\text{C}$. Note: PPg, grafted polypropylene.

temperature, a constant factor a_T was needed to shift the data at all frequencies. However, to build master curves of the BPPs, different values of a_T factors were needed at each phase angle, $a_T(\delta)$.

The fitting of the a_T coefficients of PPg to the Arrhenius model^[40] gives a flow activation energy, E_a , of 39.5 kJ mol^{-1} . This value is similar to those reported by other authors for lineal PP.^[3,7,15,46] Similarly, the fitting of the $a_T(\delta)$ coefficients of the BPPs to the Arrhenius model gives a flow activation energy that is a function of the phase angle. Figure 9 displays the values of E_a for the polymers in Figure 8. The trend of this parameter is to decrease as the phase angle decreases (increasing frequencies) approaching the activation energy of the linear material. The new high molecular weight complex molecules, with their longer relaxation times, affect mainly the flow at low frequencies, as already commented, and display larger flow activation energies. This behavior has already been observed for branched PPs, in which E_a up to 100 kJ mol^{-1} have been calculated at low frequencies.^[1,3,7,8,12,15]

Thermal analysis

The effect of the molecular structure on the thermal behavior of the polymers was analyzed by differential scanning calorimetry. Figure 10 displays the exotherms of crystallization of all materials obtained at $10^\circ\text{C min}^{-1}$. For small doses of CA, the crystallization process of the BPPs is practically equal or slightly shifted to lower temperatures, compare to that of PPg. As the CA concentration increases, the B-, E-, and P-families

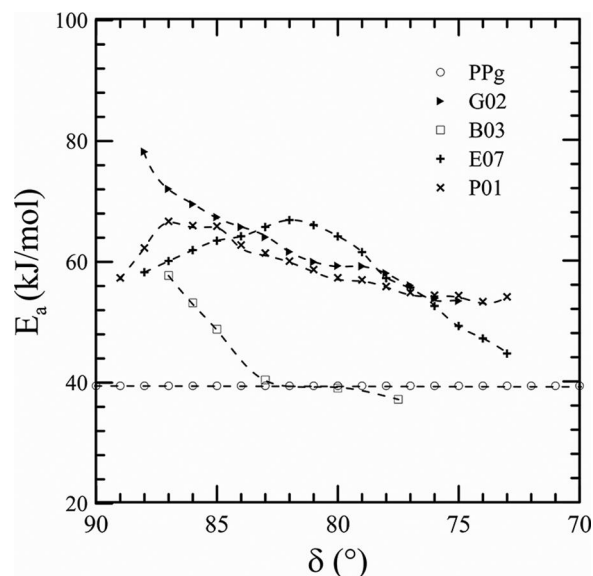


Figure 9. Flow activation energy of the polymers in Figure 8.

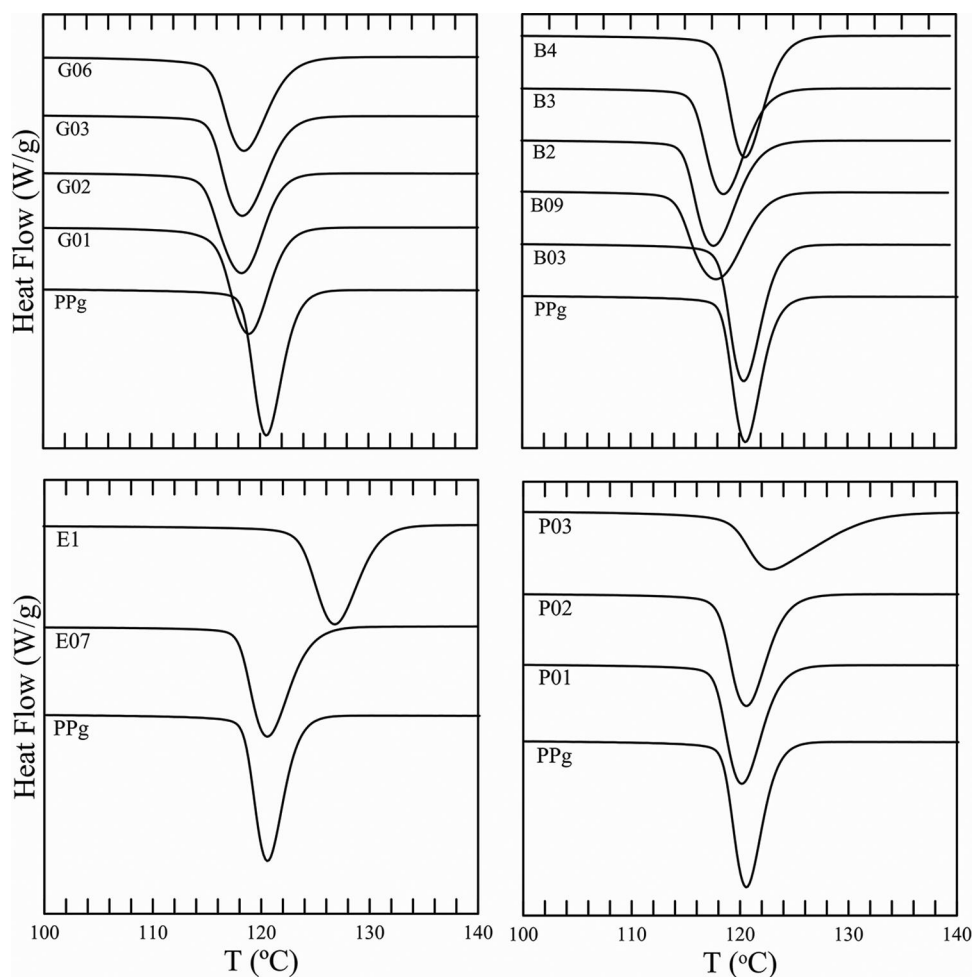


Figure 10. Thermograms of crystallization of PPg and BPPs obtained at $10^{\circ}\text{C min}^{-1}$. Note: PPg, grafted polypropylene; BPP, branched polypropylene.

of BPPs display a tendency to crystallize at slightly higher temperatures. Table 4 lists the values of the crystallization temperature (T_c), obtained from the maxima of the exotherm, as well as the onset temperature of crystallization ($T_{c,\text{onset}}$), which is calculated when 1% of the material has crystallized. All data in

this table correspond to the average of at least three thermograms. Also listed in Table 4 are the melting temperature (T_m), obtained from the maxima of the endotherm measured at $10^{\circ}\text{C min}^{-1}$, and the crystallization (ΔH_c) and melting (ΔH_m) enthalpies. It can be observed that most BPPs display T_m and ΔH_m slightly

Table 4. Thermal properties of all polymers.

	T_f (°C)	$T_{c,\text{onset}}$ (°C)	T_c (°C)	ΔH_f (J g^{-1})	ΔH_c (J g^{-1})	$t_{1/2}$ (min)	ΔE_x at $\chi = 0.2$	ΔE_x at $\chi = 0.4$
PPg	161	125	120	105	101	0.50	-290	-280
G01	159	124	119	104	96	0.48	-295	-280
G02	158	123	118	103	96	0.48	-300	-280
G03	159	124	118	102	97	0.55	-255	-230
G06	158	125	119	106	93	0.58	-240	-195
B03	159	125	121	99	98	0.43	-235	-205
B09	158	124	118	100	98	0.60	-230	-205
B2	157	124	118	98	99	0.60	-225	-215
B3	157	124	119	98	97	0.52	-225	-205
B4	159	126	121	100	100	0.50	-245	-225
E07	159	127	121	102	99	0.56	-275	-260
E1	162	132	127	105	100	0.57	-235	-215
P01	160	126	120	102	97	0.52	-245	-215
P02	159	126	121	100	96	0.56	-185	-165
P03	161	135	123	102	95	1.06	-230	-210

smaller than those of PPg without showing a special trend with CA concentration.

Regarding the crystallization process, PPg displays a T_c that is 5–10°C larger than most reported values of isotactic PP.^[21,47–49] This difference has been associated to the nucleating effect of the AGs. With respect to ΔH_c , its value is similar to those reported for isotactic PP.^[21,49] As commented above, the BPPs obtained with G and B have T_c and $T_{c,onset}$ similar or slightly lower than those of PPg, being the shift not larger than 2°C. The use of the smaller doses of E and P gives place to materials that display slightly larger T_c and $T_{c,onset}$ than PPg (~1°C). An increase in CA concentration produces a larger augment in T_c of both types of materials (7°C in E1 and 3°C in P03) with an increment in the crystallization temperature range of P03. The presence of fractions of high molecular weight material in this polymer may be the cause of this distinct behavior. The same qualitative behavior was observed when larger doses of glycerol and epoxy were used, producing fractions of highly crosslinked material in the BPPs.^[26,27] According to most works in the literature, the T_c of BPPs is larger than that of linear PP and augments with the degree of modification.^[1,18–21,48,50] This behavior is associated to the nucleating effect of the long-chain branches. The small increase in T_c , and even slight decrease, observed in the BPPs studied in this work in comparison with the results in the literature may be due to the use of a PPg as the pristine polymer instead of a PP. In this way, a compensating effect may be occurring between the nucleating effect of the AGs remaining in the BPPs and those of the generated complex molecules. For example, the behavior of the B-family can be explained by the decrease in AG concentration (Figure 2) and the low level of branching achieved (which does not compensate the smaller concentration of AG). However, for equivalent remaining AGs in the E- and P- families, the value of T_c agrees with a larger branching level.

Table 4 also lists the value of the crystallization half-time, $t_{1/2}$, which is the time at which the materials reach 50% of their final crystallinity (crystallization enthalpy ratio, χ , equal to 0.5). The crystallization enthalpy ratio corresponds to the accumulative integration of the endotherms of crystallization divided by ΔH_c , while the time is calculated as

$$t = \frac{T_{c,onset} - T}{\Phi} \quad (5)$$

In this equation, T is the temperature and Φ is the cooling rate. The data in Table 4 were obtained using $\Phi = 10^\circ\text{C min}^{-1}$. It can be observed that, except in the case of P03, $t_{1/2}$ of the BPPs is just slightly larger (slower crystallization rate) than that of PPg and does

not show a special trend. The larger value of $t_{1/2}$ of P03 agrees with previous results of BPPs obtained with G and E that present fractions of gel-like material.^[26,27]

The activation energy of crystallization, ΔE_χ , can then be determined from the exotherms obtained at different cooling rates. For example, according to the methodology proposed by Friedman and Vyazokin,^[51,52] ΔE_χ can be calculated from

$$\ln\left(\frac{d\chi}{dt}\right)_\chi = \text{Cte} - \frac{\Delta E_\chi}{RT_\chi} \quad (6)$$

where $(d\chi/dt)_\chi$ is the derivative of the crystallization enthalpy ratio with respect to time at a given value of crystallization enthalpy ratio, R is the universal gas constant, and T_χ is the temperature at which that χ is reached. That is, the slopes of the curves of χ as a function of time at each cooling rate calculated, at a given crystallization enthalpy ratio, plotted against $1/T_\chi$ allows to determine ΔE_χ . This energy can be interpreted as a measure of the difficulty in the crystallization process considering simultaneously the generation of crystallization nuclei and the diffusion into these nuclei.

Table 4 displays the values of ΔE_χ at two crystallization enthalpy ratios, $\chi = 0.2$ and 0.4 . All values are negative and in a range that indicates the crystallization process is dominated by nucleation. The ΔE_χ of PPg is smaller than values reported in the literature for isotactic PP, which are in the range of -240 to -180 kJ mol^{-1} at $\chi = 0.2$.^[48,53,54] The presence of the AGs, with their nucleating effect, justifies the faster crystallization process of PPg with respect to PP. The augment in the value of ΔE_χ displayed by the BPPs as they get more modified shows that the diffusion of the macromolecules gets gradually more important relative to the nucleation process, hindering the crystallization. Within the range of crystallization considered, the influence of the transport phenomena can also be seen in the activation energy of crystallization of each polymer, that increases with χ . Tian et al.^[48] have reported ΔE_χ of approximately -240 kJ mol^{-1} at $\chi = 0.2$ for three branched PPs, which is in the range of values reported here.

Conclusion

The physicochemical analysis, through IR spectra, of the synthesized materials demonstrates that the maleic anhydride functionalized PP reacts with all the considered chain-linking agents. However, the concurrent analysis by SEC with LS, RI, and IV detectors and dynamic rheological measurements confirm the existence of branched molecular structure in all synthesized materials that becomes more complex as

the chain-linking agent concentration increases. The presence of long-chain branches, however, practically does not affect the crystallization process of PPg.

A comparative analysis of the properties of the BPPs shows that 1,4-phenylenediamine is the most efficient chain-linking agent. This agent produces the largest degree of branching at significantly lower concentrations than the other three modifiers, and gives place to BPPs more uniformly modified, with better homogeneous distribution of branches in the polymer. Moreover, the introduction of branches enhances the elastic behavior of the linear PPg, giving place to thermorheologically complex properties.

Acknowledgment

The authors wish to thank CONICET, ANPCyT, and the Universidad Nacional del Sur for the financial support.

Funding

This work was supported by the Agencia Nacional de Promoción Científica y Tecnológica [Grant Number PICT 2013-1108], Consejo Nacional de Investigaciones Científicas y Técnicas [Grant Number 112-201301-00708-CO], and Universidad Nacional del Sur [Grant Number 24/M145].

ORCID

Lidia M. Quinzani  <http://orcid.org/0000-0002-4040-4865>

References

- [1] Nam, G. J.; Yoo, J. H.; Lee, J. W. Effect of Long-Chain Branches of Polypropylene on Rheological Properties and Foam-Extrusion Performances. *J. Appl. Polym. Sci.* **2005**, *96*, 1793–1800. DOI:10.1002/app.21619
- [2] Krause, B.; Voigt, D.; Häußler, L.; Auhl, D.; Münstedt, H. Characterization of Electron Beam Irradiated Polypropylene: Influence of Irradiation Temperature on Molecular and Rheological Properties. *J. Appl. Polym. Sci.* **2006**, *100*, 2770–2780. DOI:10.1002/app.23453
- [3] Langston, J. A.; Colby, R. H.; Chung, T. C. M.; Shimizu, F.; Suzuki, T.; Aoki, M. Synthesis and Characterization of Long Chain Branched Isotactic Polypropylene via Metallocene Catalyst and T-Reagent. *Macromolecules* **2007**, *40*, 2712–2720. DOI:10.1021/ma062111+
- [4] El Mabrouk, K.; Parent, J. S.; Chaudhary, B. I.; Cong, R. Chemical Modification of PP Architecture: Strategies for Introducing Long-Chain Branching. *Polymer* **2009**, *50*, 5390–5397. DOI:10.1016/j.polymer.2009.09.066
- [5] Su, F. H.; Huang, H. X. Supercritical Carbon Dioxide-Assisted Reactive Extrusion for Preparation Long-Chain Branching Polypropylene and Its Rheology. *J. Supercrit. Fluids* **2011**, *56*, 114–120. DOI:10.1016/j.supflu.2010.12.001

- [6] Wan, D.; Ma, L.; Xing, H.; Wang, L.; Zhang, Z.; Qiu, J.; Zhang, G.; Tang, T. Preparation and Characterization of Long Chain Branched Polypropylene Mediated by Different Heteroaromatic Ring Derivatives. *Polymer* **2013**, *54*, 639–651. DOI:10.1016/j.polymer.2012.12.014
- [7] Paavola, S.; Saarinen, T.; Löfgren, B.; Pitkänen, P. Propylene Copolymerization with Non-Conjugated Dienes and α -Olefins Using Supported Metallocene Catalyst. *Polymer* **2004**, *45*, 2099–2110. DOI:10.1016/j.polymer.2004.01.053
- [8] Ye, Z.; Alobaidi, F.; Zhu, S. Synthesis and Rheological Properties of Long-Chain-Branched Isotactic Polypropylenes P Prepared by Copolymerization of Propylene and Nonconjugated Dienes. *Ind. Eng. Chem. Res.* **2004**, *43*, 2860–2870.
- [9] Langston, J. A.; Dong, J. Y.; Chung, T. C. One-Pot Process of Preparing Long Chain Branched Polypropylene Using C-Symmetric Metallocene Complex and a “T” Reagent. *Macromolecules* **2005**, *38*, 5849–5853. DOI:10.1021/ma0506841
- [10] Zhang, Z.; Wan, D.; Xing, H.; Zhang, Z.; Tan, H.; Wang, L.; Zheng, J.; An, Y.; Tang, T. A New Grafting Monomer for Synthesizing Long Chain Branched Polypropylene through Melt Radical Reaction. *Polymer* **2012**, *53*, 121–129.
- [11] Guo, P.; Xu, Y.; Lu, M.; Zhang, S. High Melt Strength Polypropylene with Wide Molecular Weight Distribution Used as Basic Resin for Expanded Polypropylene Beads. *Ind. Eng. Chem. Res.* **2015**, *54*, 217–225. DOI:10.1021/ie503503k
- [12] Sugimoto, M.; Tanaka, T.; Masubuchi, Y.; Takimoto, J.; Koyama, K. Effect of Chain Structure on the Melt Rheology of Modified Polypropylene. *J. Appl. Polym. Sci.* **1998**, *73*, 1493–1500. DOI:10.1002/(sici)1097-4628(19990822)73:8<1493::aid-app18>3.0.co;2-2
- [13] Yoshiga, A.; Otaguro, H.; Parra, D. F.; Lima, L. F. C. P.; Lugao, A. B. Controlled Degradation and Crosslinking of Polypropylene Induced by Gamma Radiation and Acetylene. *Polym. Bull.* **2009**, *63*(3), 397–409. DOI:10.1007/s00289-009-0102-7
- [14] Amintowli, Y.; Tzoganakis, C.; Penlidis, A. An Overview of the Potential of UV Modification of Polypropylene. *Macromol. Symp.* **2016**, *360*, 96–107. DOI:10.1002/masy.201500110
- [15] Rätzsch, M.; Arnold, M.; Borsig, E.; Bucka, H.; Reichelt, N. Radical Reactions on Polypropylene in the Solid State. *Prog. Polym. Sci.* **2002**, *27*, 1195–1282. DOI:10.1016/s0079-6700(02)00006-0
- [16] Borsig, E.; van Duin, M.; Gotsis, A. D.; Picchioni, F. Long Chain Branching on Linear Polypropylene by Solid State Reactions. *Eur. Polym. J.* **2008**, *44*, 200–212. DOI:10.1016/j.eurpolymj.2007.10.008
- [17] Köster, M.; Hellmann, G. P. Chain Extension of Maleinated Poly(Propylene) by Reactive Extrusion. *Macromol. Mater. Eng.* **2001**, *286*, 769–773.
- [18] Graebing, D. Synthesis of Branched Polypropylene by a Reactive Extrusion Process. *Macromolecules* **2002**, *35*, 4602–4610. DOI:10.1021/ma0109469
- [19] Tang, H.; Dai, W.; Chen, B. A New Method for Producing High Melt Strength Polypropylene With Reactive Extrusion. *Polym. Eng. Sci.* **2008**, *48*, 1339–1344.

- [20] Li, S.; Xiao, M.; Wei, D.; Xiao, H.; Hu, F.; Zheng, A. The Melt Grafting Preparation and Rheological Characterization of Long Chain Branching Polypropylene. *Polymer* **2009**, *50*, 6121–6128. DOI:10.1016/j.polymer.2009.10.006
- [21] Su, F. H.; Huang, H. X. Rheology and Thermal Behavior of Long Branching Polypropylene Prepared by Reactive Extrusion. *J. Appl. Polym. Sci.* **2009**, *113*, 2126–2135. DOI:10.1002/app.30061
- [22] Su, F. H.; Huang, H. Influence of Polyfunctional Monomer on Melt Strength and Rheology of Long-Chain Branched Polypropylene by Reactive Extrusion. *J. Appl. Polym. Sci.* **2010**, *116*, 2557–2565.
- [23] Cao, K.; Li, Y.; Lu, Z.; Wu, S.; Chen, Z.; Yao, Z. Preparation and Characterization of High Melt Strength Polypropylene with Long Chain Branched Structure by the Reactive Extrusion Process. *J. Appl. Polym. Sci.* **2011**, *121*, 3384–3392. DOI:10.1002/app.34007
- [24] Zhang, W.; Yang, L.; Chen, P.; Zhang, H.; Lin, W.; Wang, Y. Preparation of Long-Chain Branching Polypropylene and Investigation on Its Foamability. *Polym. Eng. Sci.* **2013**, *53*, 1598–1604. DOI:10.1002/pen.23416
- [25] Wang, K.; Wang, S.; Wu, F.; Pang, Y.; Liu, W.; Zhai, W.; Zheng, W. A New Strategy for Preparation of Long-Chain Branched Polypropylene via Reactive Extrusion with Supercritical CO₂ Designed for an Improved Foaming Approach. *J. Mater. Sci.* **2016**, *51*, 2705–2715. DOI:10.1007/s10853-015-9584-x
- [26] Guapacha, J.; Vallés, E. M.; Quinzani, L. M.; Failla, M. D. Long-Chain Branched Polypropylene Obtained Using an Epoxy Resin as Crosslinking Agent. *Polym. Bull.* **2016**, *74*, 2297–2318. DOI:10.1007/s00289-016-1839-4
- [27] Guapacha, J.; Failla, M. D.; Vallés, E. M.; Quinzani, L. M. Molecular, Rheological, and Thermal Study of Long-Chain Branched Polypropylene Obtained by Esterification of Anhydride Grafted Polypropylene. *J. Appl. Polym. Sci.* **2014**, *131*, 40357.
- [28] Matuana, L. M.; Balatinez, J. J.; Sodhi, R. N. S.; Park, C. B. Surface Characterization of Esterified Cellulosic Fibers by XPS and FTIR Spectroscopy. *Wood Sci. Technol.* **2001**, *35*, 191–201. DOI:10.1007/s002260100097
- [29] Socrates, G. *Infrared and Raman Characteristic Group Frequencies*, 3rd ed.; John Wiley & Sons: New York, 2001.
- [30] Muñoz, P. A. R.; Bettini, S. H. P. Assessment of the Utilization of Different Peroxide Dispersion Media on the Controlled Degradation of Polypropylene. *J. Appl. Polym. Sci.* **2013**, *127*, 87–95. DOI:10.1002/app.36705
- [31] Lou, J.; Luo, Z.; Li, Y. The Effect of Epoxy and Tetramethyl Thiuram Disulfide on Melt-Grafting of Maleic Anhydride onto Polypropylene by Reactive Extrusion. *J. Appl. Polym. Sci.* **2016**, *133*, 43422.
- [32] Scholte, T. G.; Meijerink, N. L. J.; Schoffeleers, H. M.; Brands, A. M. G. Mark–Houwink Equation and GPC Calibration Linear Short-Chain Branched Polyolefins, Including Polypropylene and Ethylene–Propylene Copolymers. *J. Appl. Polym. Sci.* **1984**, *29*, 3763–3782. DOI:10.1002/app.1984.070291211
- [33] Zimm, B. H.; Stockmayer, W. H. The Dimensions of Chain Molecules Containing Branches and Rings. *J. Chem. Phys.* **1949**, *17*, 1301–1314. DOI:10.1063/1.1747157
- [34] Zimm, B. H.; Kilb, R. W. Dynamics of Branched Polymer Molecules in Dilute Solution. *J. Polym. Sci.* **1959**, *37*, 19–42.
- [35] Lecacheux, D.; Lesec, J.; Quivoron, C. High-Temperature Coupling of High-Speed GPC with Continuous Viscometry. II. Long-Chain Branching in Polyethylene. *J. Appl. Polym. Sci.* **1982**, *27*, 4867–4877. DOI:10.1002/app.1982.070271231
- [36] Legendijk, R. P.; Hogt, A. H.; Buijtenhuijs, A.; Gotsis, A. D. Peroxydicarbonate Modification of Polypropylene and Extensional Flow Properties. *Polymer* **2001**, *42*(25), 10035–10043. DOI:10.1016/s0032-3861(01)00553-5
- [37] Li, Y.; Yao, Z.; Chen, Z.; Qiu, S.; Zeng, C.; Cao, K. Rheological Evidence of Physical Cross-Links and Their Impact in Modified Polypropylene. *Ind. Eng. Chem. Res.* **2013**, *52*, 7758–7767. DOI:10.1021/ie400809z
- [38] Gotsis, A. D.; Zeevenhoven, B. L. F.; Hogt, A. H. The Effect of Long Chain Branching on the Processability of Polypropylene in Thermoforming. *Polym. Eng. Sci.* **2004**, *44*(5), 973–982. DOI:10.1002/pen.20089
- [39] Tian, J.; Yu, W.; Zhou, C. The Preparation and Rheology Characterization of Long Chain Branching Polypropylene. *Polymer* **2006**, *47*, 7962–7969. DOI:10.1016/j.polymer.2006.09.042
- [40] Han, C. D. *Rheology and Processing of Polymeric Materials: Polymer Rheology*; Oxford University Press: New York, 2007, Vol. 1
- [41] Graessley, W. W. *Polymeric Liquids and Networks: Dynamics and Rheology*; Garland Science: London, 2008.
- [42] Auhl, D.; Stadler, F. J.; Münstedt, H. Comparison of Molecular Structure and Rheological Properties of Electron-Beam and Gamma-Irradiated Polypropylene. *Macromolecules* **2012**, *45*(4), 2057–2065. DOI:10.1021/ma202265w
- [43] Raps, D.; Köppl, T.; Heymann, L.; Altstädt, V. Rheological Behaviour of a High-Melt-Strength Polypropylene at Elevated Pressure and Gas Loading for Foaming Purposes. *Rheol. Acta* **2017**, *56*, 95–111. DOI:10.1007/s00397-016-0988-6
- [44] Vega, J. F.; Expósito, M. T.; Martínez-Salazar, J.; Lobón-Poo, M.; Barcina, J. O.; Martínez, A. G.; López, M. Molecular Architecture and Linear Viscoelasticity of Homogeneous Ethylene/styrene Copolymers. *Rheol. Acta* **2011**, *50*(3), 207–220. DOI:10.1007/s00397-010-0521-2
- [45] Keßner, U.; Münstedt, H. Thermorheology as a Method to Analyze Long-Chain Branched Polyethylenes. *Polymer* **2010**, *51*(2), 507.
- [46] Gahleitner, M. Melt Rheology of Polyolefins. *Prog. Polym. Sci.* **2001**, *26*, 895–944. DOI:10.1016/s0079-6700(01)00011-9
- [47] Seo, Y.; Kim, J.; Kim, K. U.; Kim, Y. C. Study of the Crystallization Behaviors of Polypropylene and Maleic Anhydride Grafted Polypropylene. *Polymer* **2000**, *41*, 2639–2646. DOI:10.1016/s0032-3861(99)00425-5
- [48] Tian, J.; Yu, W.; Zhou, C. Crystallization Behaviors of Linear and Long Chain Branched Polypropylene. *J. Appl. Polym. Sci.* **2007**, *104*, 3592–3600. DOI:10.1002/app.26024
- [49] Berzin, F.; Flat, J. J.; Vergnes, B. Grafting of Maleic Anhydride on Polypropylene by Reactive

- Extrusion: Effect of Maleic Anhydride and Peroxide Concentrations on Reaction Yield and Products Characteristics. *J. Polym. Eng.* **2013**, 33(8), 673–682.
- [50] Zhou, S.; Wang, W.; Xin, Z.; Zhao, S.; Shi, Y. Relationship Between Molecular Structure, Crystallization Behavior, and Mechanical Properties of Long Chain Branching Polypropylene. *J. Mater. Sci.* **2016**, 51, 5598–5608. DOI:10.1007/s10853-016-9856-0
- [51] Vyazovkin, S. Is the Kissinger Equation Applicable to the Processes that Occur on Cooling? *Macromol. Rapid Commun.* **2002**, 23(13), 771–775.
- [52] Yang, B.; Yang, M.; Wen-Jun, W.; Zhu, S. Effect of Long Chain Branching on Non-Isothermal Crystallization Behavior of Polyethylenes Synthesized with Constrained Geometry Catalyst. *Polym. Eng. Sci.* **2012**, 52, 21–34. DOI:10.1002/pen.22040
- [53] Lonkar, S. P.; Morlat-Therias, S.; Caperaa, N.; Leroux, F.; Gardette, J. L.; Singh, R. P. Preparation and Nonisothermal Crystallization Behavior of Polypropylene/Layered Double Hydroxide Nanocomposites. *Polymer* **2009**, 50, 1505–1515. DOI:10.1016/j.polymer.2009.01.031
- [54] Ardanuy, M.; Velasco, J. I.; Realinho, V.; Arencón, D.; Martínez, A. B. Non-Isothermal Crystallization Kinetics and Activity of Filler in Polypropylene/Mg–Al Layered Double Hydroxide Nanocomposites. *Thermochim. Acta* **2008**, 479, 45–52. DOI:10.1016/j.tca.2008.09.016